PERGAMON

Journal of Structural Geology 24 (2002) 1327–1344

JOURNAL OF STRUCTURAL GEOLOGY

www.elsevier.com/locate/jstrugeo

First evidence for high-grade, Himalayan-age synconvergent extension recognised within the western syntaxis—Nanga Parbat, Pakistan

T.W. Argles[a,*], M.A. Edwards[b,c]

[a]*Department of Earth Sciences, Open University, Milton Keynes MK7 6AA, UK*
[b]*Department of Geological Sciences, State University of New York at Albany, 1400 Washington Avenue, Albany, NY 12222, USA*
[c]*Asian Tectonics Research Unit, Institüt für Geologie, TU–Bergakademie Freiberg, D-09596 Freiberg, Germany*

Received 7 December 2000; revised 24 August 2001; accepted 9 October 2001

Abstract

We present evidence for horizons of medium to high grade (400–600°C) deformation accompanying normal sense displacement in high-strain Himalayan gneisses and schists from the southeastern Nanga Parbat massif, the western syntaxis in the Pakistan Himalaya. In their present orientation, the broadly N–S trending, steeply-dipping gneisses show microstructural and outcrop scale evidence for dextral and sinistral shear in discrete layers. We interpret these as horizons of thrust and normal motion within the footwall of the original Main Mantle Thrust, once Neogene antiformal folding is removed. This is the first report of significant normal motion in the Main Mantle Thrust footwall in the Nanga Parbat syntaxis and may indicate that synconvergent extension in the Himalaya extended to the western syntaxis. This episode of extension could correspond to a period of similar normal motion in the central Himalaya, or represent a separate event earlier in the orogeny.

Keywords: Nanga Parbat syntaxis; Ductile extension; Himalayas; Main Mantle Thrust; Shear sense

1. Introduction

The Himalayan mountain chain is a prime example of continental collision and provides essential insight into active or recent structural features and tectonic processes that facilitate their recognition in older orogens. The phenomenon of synconvergent extension where extension and convergence directions are co-parallel was first clearly documented in the Himalaya/southern Tibet (Burg et al., 1984) in the form of a large, low-angle detachment and accompanying metamorphic/stratigraphic break. This post-Miocene structure (now termed the Southern Tibet Detachment System—STDS) has since been recognised at intervals all along the main high Himalaya (Herren, 1987; Pêcher, 1991; Burchfiel et al., 1992; Edwards et al., 1996). Despite this widespread recognition, however, there has hitherto been little evidence from the western syntaxis of significant normal sense displacement at medium to high grade conditions related to the initial stages of exhumation of the Indian plate.

In the northwest Himalaya (Fig. 1), much of the Himalayan shortening is accommodated along the Main Mantle Thrust (MMT), also known as the Indus suture. The MMT is the collisional suture, tilted to the orientation of a moderately N-dipping reverse fault, whose hanging wall, the Kohistan Ladakh Series (KLS), represents a Cretaceous island arc trapped between India and Asia in this part of the Himalayan orogen (Tahirkheli and Jan, 1979; Bard, 1983). It is of interest that the highest pressure rocks in the Himalaya (eclogites; e.g. Pognante and Spencer, 1991; Guillot et al., 1997; O'Brien et al., 2001) occur in the western Himalaya, generally just south of the suture (Fig. 1), though no eclogites of comparable pressures occur in the Nanga Parbat–Haramosh Massif (NPHM) itself. Additionally, the STDS has not been traced into the NW Himalaya, and interpretation of previous mapping (e.g. Wadia, 1931; Gansser, 1964) suggests that the STDS does not extend significantly west of Zanskar. Although some local, lower temperature, extensional shears with top-to-the-N displacement (Treloar et al., 1991a; Vince and Treloar, 1996), and a region of extensional collapse folding (Burg et al., 1996) have been documented in the MMT footwall west of the syntaxis, we present in this paper the first report of normal sense displacement associated with deformation under medium to high grade conditions.

* Corresponding author. Tel.: +44-1908-858509; fax: +44-1908-655151.

E-mail addresses: t.w.argles@open.ac.uk (T.W. Argles), edwards@geo.tu-freiberg.de (M.A. Edwards).

0191-8141/02/$ - see front matter
PII: S0191-8141(01)00136-5

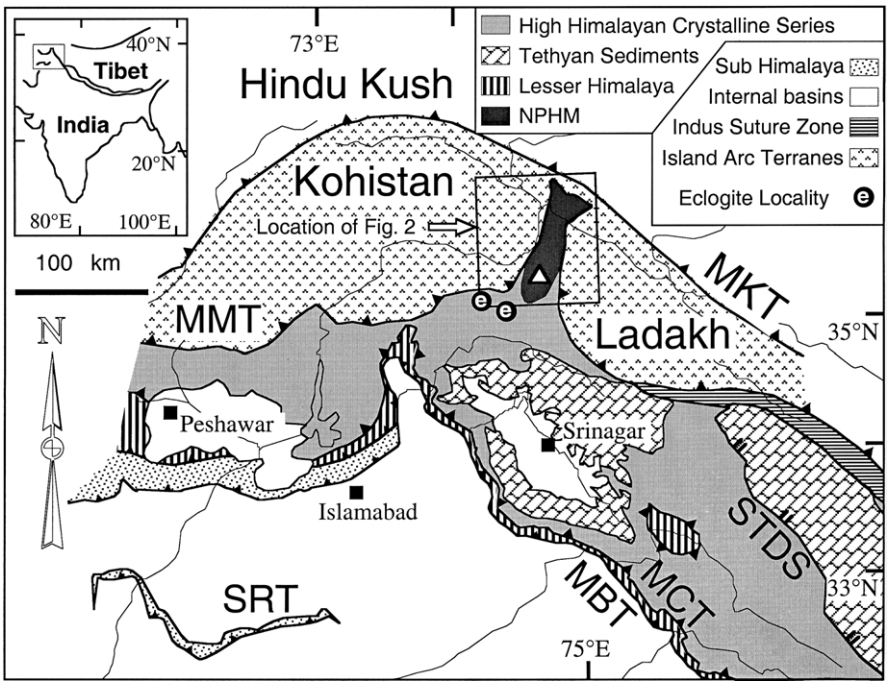

Fig. 1. Regional Map of northwest Himalaya. MKT—Main Karakoram Thrust; MMT—Main Mantle Thrust; SRT—Salt Range Thrust; STDS—Southern Tibet Detachment System (section shown is Zanskar Shear Zone); MCT—Main Central Thrust; MBT—Main Boundary Thrust. NPHM—Nanga Parbat Haramosh Massif (western Himalayan syntaxis). Inset shows location of main figure (box) with respect to India and Himalaya. Compiled from Gansser (1964), Coward et al. (1988), Searle et al. (1988) and Greco and Spencer (1993).

2. Overview of the NPHM

The western syntaxis (Wadia, 1931, 1932) marks the limit of the Himalayan belt *sensu stricto,* and the northernmost exposure of Indian-plate rocks, the NPHM (Fig. 2). The NPHM–KLS contact forms an 'oxbow' shape in plan-view around the NPHM (Coward et al., 1986; Butler et al., 1992; Lemennicier et al., 1996; Pêcher and Le Fort, 1998), and it is locally modified or cut out on the NPHM's western flank by subsequent E-side up and dextral strike-slip faulting (e.g. Lawrence and Schroder, 1984; Madin 1986; Butler et al., 1989; Madin et al., 1989; Owen, 1989; Butler et al., 1992). Various studies have shown that the MMT's oxbow trace is not the result of an Indian promontory acting as an indenter (Butler et al., 1992; Lemennicier et al., 1996; Pêcher and Le Fort, 1998), but due to crustal-scale anti-formal folding (Gansser, 1964; Coward, 1985; Coward et al., 1986) attested to by several NNE-trending fold axes in the W–E Indus Gorge section (Madin 1986; Madin et al., 1989; Treloar et al., 1991b; Butler et al., 1992; Wheeler et al., 1995), and the Burdish Ridge and Dichil antiforms in the Astor River Gorge (Figs. 3 and 4; Edwards, 1998). Deflection of the MMT trace around the NPHM has resulted in a diverse nomenclature for the eastern continuation of the MMT, including "Southern Suture" (Gansser, 1981) and "Indus–Tsangpo Suture" (Coward et al., 1986). Where the NPHM–KLS contact can be recognised as the MMT (e.g. Butler and Prior, 1988), we preserve that use of the term. In this article we restrict the term 'MMT' to the physical (lithological) contact of the Indian plate with the KLS regardless of strain. To avoid drawing an arbitrary line at the base of an 'MMT zone', we consider all Indian plate rock in the study area to be within the general MMT footwall (i.e. affected by Himalayan strain), but we focus on sections within a few kilometres only of the MMT contact.

The NPHM has drawn attention for several reasons. (1) It represents the NW terminus of the >2500 km Himalayan arc (e.g. Fielding et al., 1994). (2) It forms an anomalous spur of reworked, high grade, Indian plate Proterozoic gneisses (e.g. Chamberlain et al., 1989; Butler et al., 1992; Smith et al., 1992; Zeitler et al., 1993; Wheeler et al., 1995; Winslow et al., 1996; Schneider et al., 1999a; Whittington et al., 1999), exhumed from beneath the structural overburden of the upper Indian plate and overthrust KLS (Coward, 1985). (3) It represents an area of exceedingly recent (~0.9 to >9.0 Ma) plutonism, metamorphism and cooling (e.g. Chamberlain et al., 1989; Zeitler et al., 1993; Butler et al., 1997; Schneider et al., 1999b,c) within an area of the Himalaya where prograde metamorphism was considerably earlier (44–38 Ma (Foster et al., 2000, although cf. Schneider et al., 1999b). (4) The above Neogene events require exhumation rates of up to 5–10 mm/year (e.g. Craw et al., 1994). Unraveling the complex polyphase deformation of the NPHM, where some of the deepest structural levels in the Himalaya are exposed, is therefore central to the understanding of the evolution of the orogen. This article examines a

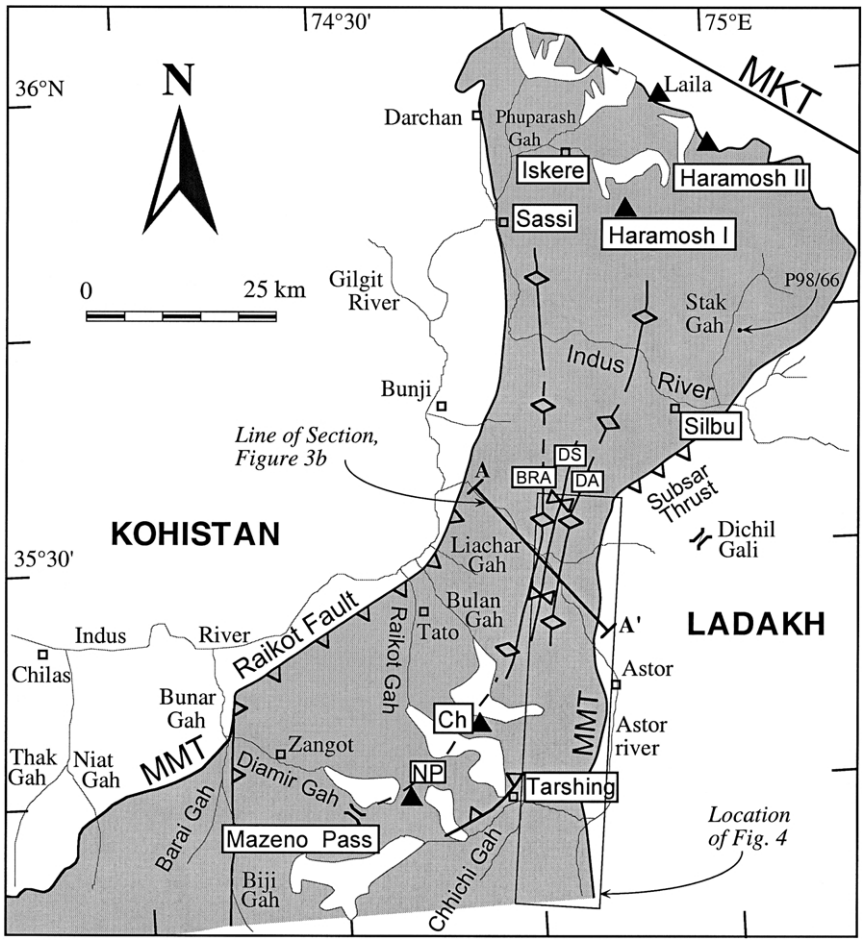

Fig. 2. Overview map of NPHM with selected valleys and towns. Grey—Indian rocks (undifferentiated); white within Indian Plate—glaciers; external white—undifferentiated KLS rocks or (north of MKT) undifferentiated Karakoram Terrane. Locality P98/66 is marked (see Fig. 7b). NP—Nanga Parbat; Ch—Chongra Northern Peak; MKT—Main Karakoram Thrust. Heavy lines with barbs—reverse faults; paired barbs represent axial traces of (W–E) Burdish Ridge Antiform, Dashkin synform, and Dichil Antiform, respectively (cf. Fig. 3). Black triangles—major peaks. Open squares—villages. Map sources: Kidd, Edwards, Asif Khan and Argles (unpublished data), Madin (1986), Madin et al. (1989), Treloar et al. (1991b), Lemennicier et al. (1996) and Pêcher and Le Fort (1998).

particular part of the NPHM's polyphase deformation: discrete normal motion during overall India–Asia convergence.

3. Himalayan deformation

In this study, we discriminate between deformation related to pre-collision events, main Himalayan events (from collision to ca. 10 Ma), and Neogene exhumation of the NPHM, whilst noting that NPHM neotectonics are a fundamental part of the continuing Himalayan collision (e.g. Seeber and Pêcher, 1998). We present evidence from the SE NPHM for two discrete deformation episodes within the main Himalayan event: thrusting followed by later normal shearing.

The main NPHM antiform and related folds affect not only the MMT and the lithological layering, but also the main amphibolite facies foliation. Hence these folds postdate the main Himalayan foliation-forming event. Reworked fabrics related to this folding event are confined to the active western margin (Liachar Thrust) and parts of the massif core. Only minimal reworking of fabrics at even the deepest structural levels (weak, localised axial-planar cleavage in some hinge zones) occurs on the eastern half of the syntaxis antiform, resulting in passive rotation of large portions of the tectonostratigraphic section (Coward et al., 1986; Edwards, 1998; Schneider et al., 1999a; Argles 2000). We apply this simple passive rotation model (Fig. 5) to the SE NPHM, assuming no significant reworking of fabric and only minor inhomogeneous strain. Earlier models for large-scale folding (e.g. Dixon, 1975; Burg, 1987) predict extensive fabric reworking, and shearing perpendicular to the fold axis. However, even after unfolding about the antiformal fold axis (01/192) as determined by the π girdle method on all foliation data (Fig. 6), lineations and shear directions in the NPHM remain predominately N–S, parallel to the major antiformal axis. This suggests

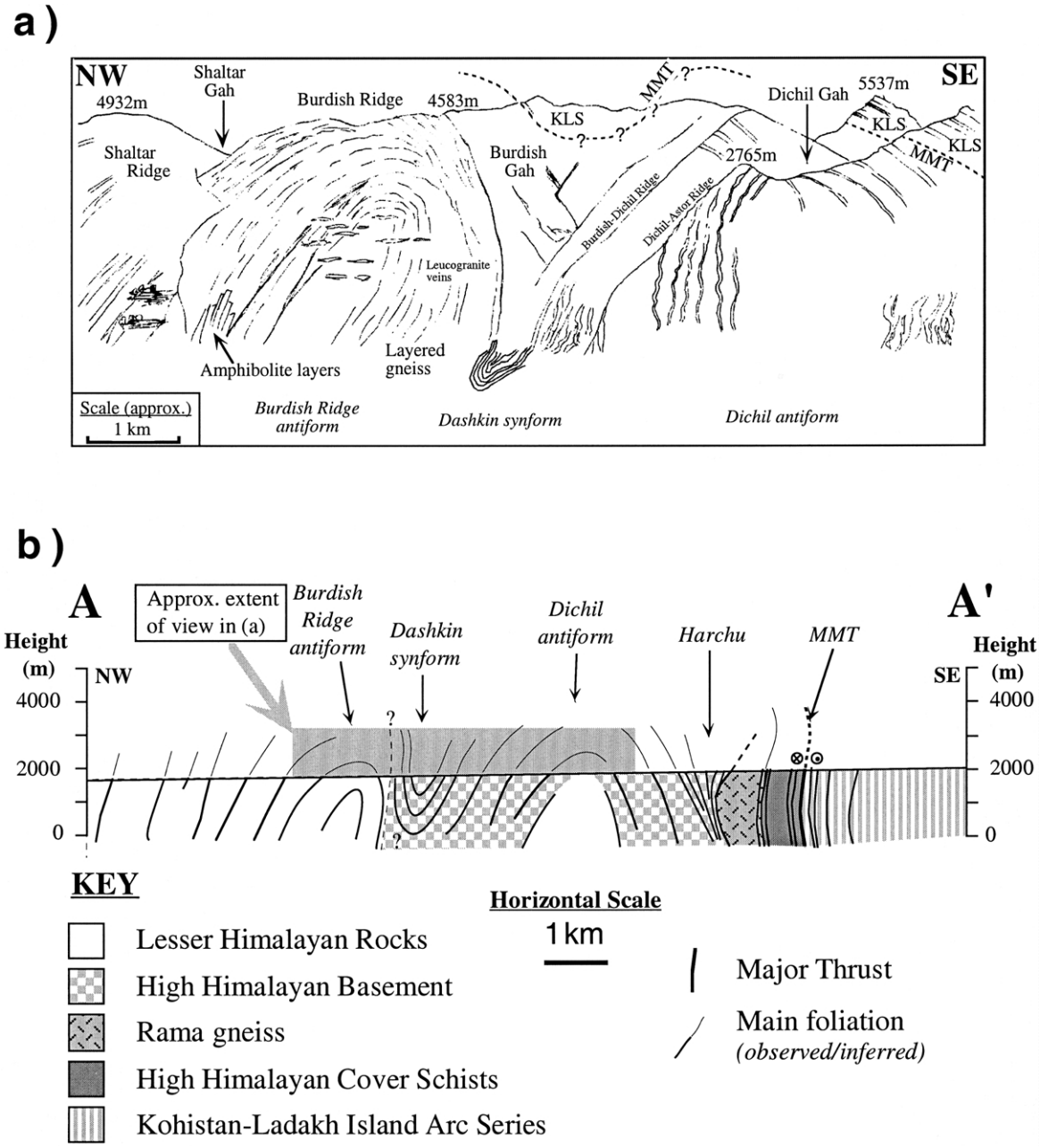

Fig. 3. Line drawing of view from Astor Gorge high road looking NE to steep walls of right bank of Astor. Gneissic layering and amphibolite-grade foliation is deformed by Burdish Ridge antiform, Dashkin synform and part of Dichil antiform. Note that limbs are generally distinct from hinge regions, and in the upper portions, KLS rocks are clearly seen to be structurally above rocks of NPHM, thereby marking the MMT. Width of view is ~10 km (see shaded box in Fig. 3b). Cross-section (for location see Fig. 2) along same transect of the view in Fig. 3a. Topographic profile corresponds to the Astor River bed, where most data were acquired. Indian plate rocks are subdivided on the basis of isotopic data (Whittington et al., 1999, 2000; Foster and Argles, in preparation), allowing better definition of the tight fold structures. The shear sense data considered in this study were mainly collected from the east limb of the Dichil antiform, where steeply-dipping to slightly overturned foliations define a conformable section sub-parallel to the MMT.

that lineations prior to syntaxial folding had mainly N–S trends, consistent with the range of principal Himalayan lineation trends (and thus original MMT motion) reported for the NW Himalaya (e.g. Chaudhry and Ghazanfar, 1987, 1990; Greco et al., 1989; Treloar et al., 1989; Burg et al., 1996).

Fig. 5 illustrates schematically how originally down-dip kinematic indicators in a high-strain fabric such as the MMT footwall foliation would acquire strike-slip geometries during essentially passive rotation onto subvertical limbs in a simple case of crustal scale antiformal folding. Fig. 5c illustrates the predicted shear sense we would observe in steep, passively rotated shear foliations following antiformal folding as in the eastern NPHM. For original

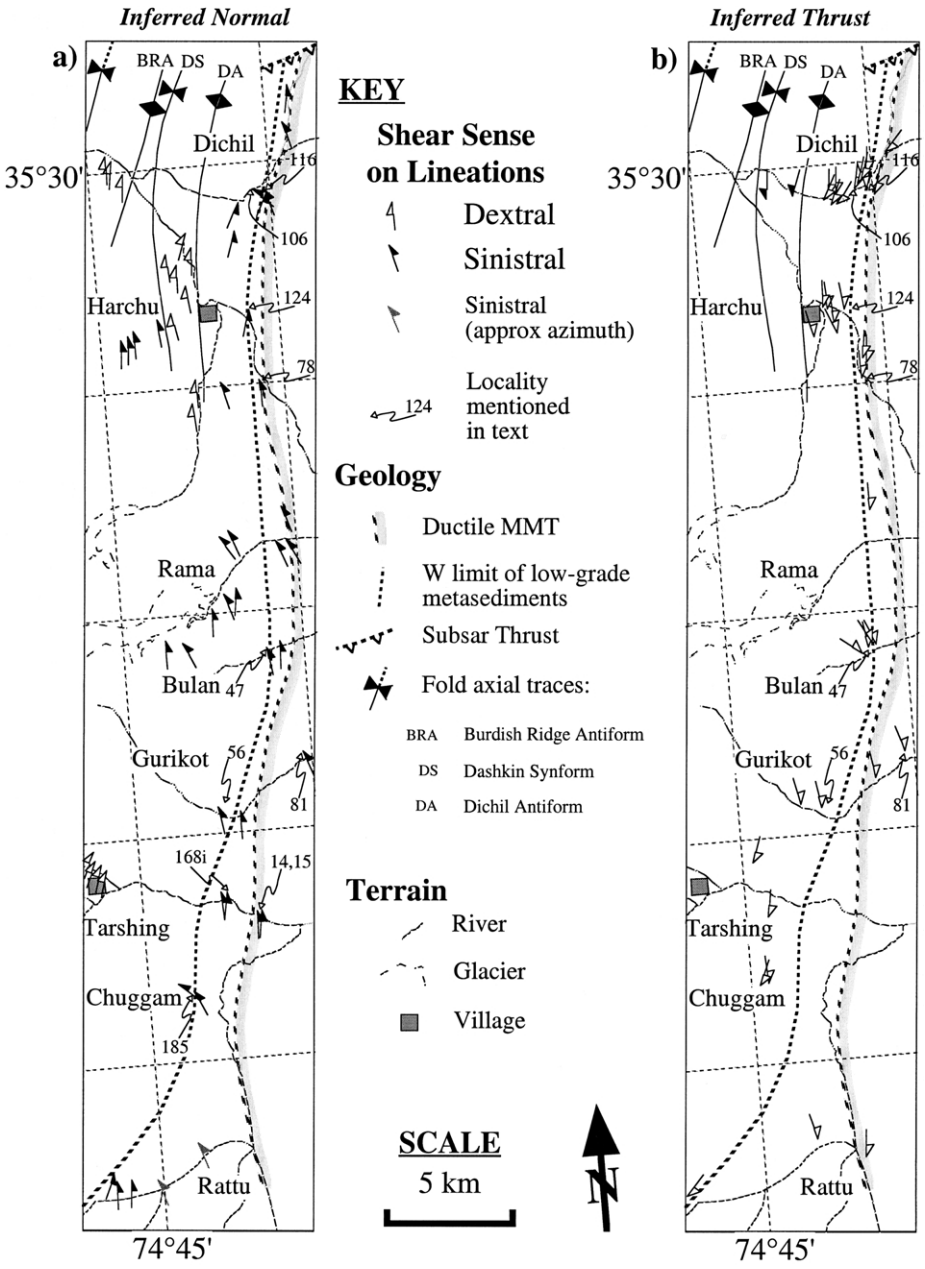

Fig. 4. Maps summarising shear sense observations in SE NPHM. Half-arrow tips indicate data localities, except where separated slightly to avoid congestion. Arrowheads point in direction of overshear, *NOT* lineation plunge (which is overwhelmingly to the north; see Fig. 6a). In each case, dextral and sinistral observations are based on the strike-slip component in present orientation, associated with the stretching lineation. Twisted arrows with labels mark localities of samples shown in Figs. 7 and 8. (a) Data inferred to represent original normal (down-dip) motion on the MMT (i.e. top-to-the-north displacement). Data fall into two main groups: in the eastern portion within the low-grade metasediments adjacent to the MMT contact, or further west in Rama Gah and in the folded section near Harchu. Note how the fold axial traces separate regions of observed dextral and sinistral shear. Data near Tarshing village are from a young (<10 Ma) shear zone related to the uplift of the Nanga Parbat summit region. (b) Data inferred to represent original thrust shearing on the MMT (i.e. top-to-the-south motion). Data are concentrated in the gneisses to the west of the low-grade metasediments, or in the hanging wall amphibolites of the MMT.

'top-to-the-south' (henceforth referred to as 'thrust') displacement criteria, dextral shear sense would be observed on the east margin, and sinistral on the west. If the opposite shear sense is preserved (e.g. sinistral on the eastern margin of the NPHM), we can infer that the original displacement was 'top-to-the-north' (henceforth referred to as 'normal' displacement).

4. Local geology

In the SE NPHM, the MMT footwall includes a series of metasedimentary schists and gneisses interlayered with marbles, amphibolites, and granitic (±migmatitic) gneisses (Fig. 7a and b), consistent with observations of NPHM rocks along the eastern Indus (Madin, 1986; Madin et al., 1989;

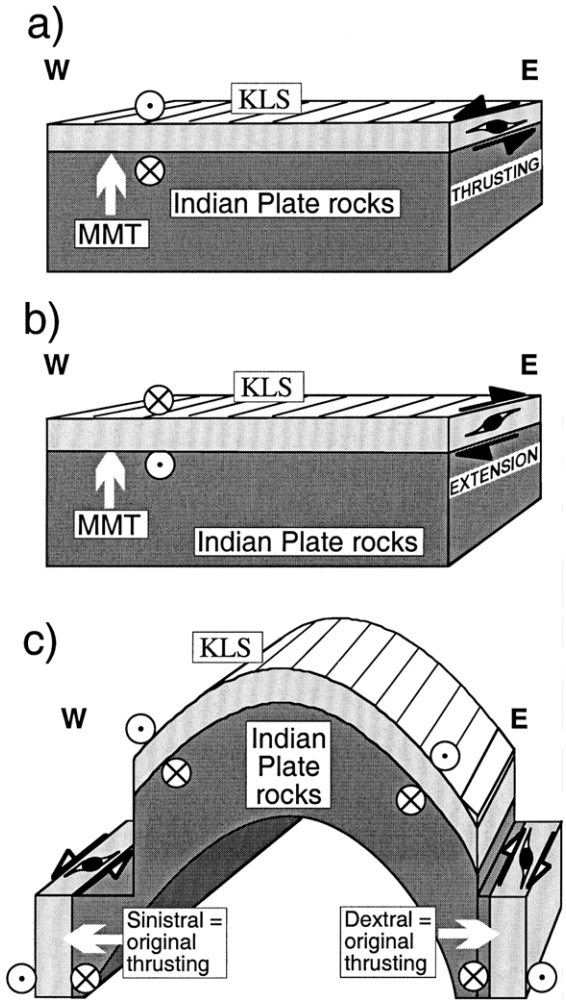

Fig. 5. (a) 3-D cross-sectional cartoon depicting initial tectonic scenario during top-to-the-S thrusting in the Indian plate. Note use of 'head and tail of arrow' symbols indicating that the hanging wall (Kohistan–Ladakh Series) has moved outward (with respect to the plane of view) while the footwall (Indian Plate) has moved inward. A thick, ductile, thrust sense, high strain horizon has developed in the MMT footwall (lighter shading with sigmoidal object symbols used as a general representation of sense of shear indicators found). (b) Same view as in (a), but showing the situation during down-dip normal shear arising from extension along the MMT, before antiformal folding. Symbols and shading as before. (c) W–E cross-sectional view of MMT after crustal scale antiformal folding. Only preserved original thrust-sense indicators are shown for clarity. Observed sense of shear from original thrust-sense indicators will be sinistral on left (west) side, dextral on right (east); vice versa for N-directed normal motion.

Treloar et al., 1991b; Wheeler et al., 1995; Pêcher and Le Fort, 1998), and from SW NPHM (Edwards, 1998; Edwards et al., 2000). KLS rocks (i.e. the MMT hanging wall) include thick sequences of amphibolite (Fig. 7c), (grano)-diorite, metabasite, and other mafic rocks, consistent with regional descriptions of the KLS rocks (Tahirkheli, 1979; Tahirkheli and Jan, 1979; Bard, 1983; Coward et al., 1988; Treloar et al., 1989).

The rocks in the first 2–4 km W of the MMT (i.e. immediate footwall) and the first few 100 m E of the MMT (hanging wall KLS section) have been divided into a series of mappable lithologies (Edwards, 1998; Argles, 2000). This overall sequence of units is broadly recognised from Dichil Gali in the north, to Chuggam Gah, ~45 km to the south. Fig. 3 (composite field sketch from Edwards, 1998) illustrates the structural style of the Astor Gorge transect; a broad antiformal fold with zones of tighter folding of the foliation. Three 'minor' (kilometre-scale) folds related to the governing antiform have been recognised (Figs. 3 and 4) on the basis of mapped closures (e.g. Mamocha Gah; Dashkin village: Fig. 3), repetition of tectonostratigraphy (Foster and Argles, in preparation), and folding of the MMT. Most of the sense of shear data presented here is from subvertical (or locally slightly overturned) foliations on the eastern limb of the Dichil antiform (Figs. 3 and 4; Edwards, 1998) on subhorizontal or shallow, mostly N-plunging lineations (Fig. 6; S-plunging lineation occur sparsely, e.g. near Tarshing and Upper Rama Gah). With these constraints, we are confident of applying the passive rotation model above to our analysis of shear sense criteria from the eastern limb of the syntaxis antiform.

5. Structural analysis

5.1. Procedures and context of shear sense observations

On well-exposed transects through the high strain rocks straddling the NPHM/KLS contact we have recorded sense of shear and identified evidence for original thrust and normal displacement related to the MMT. On the present-day steep eastern limb of the syntaxis antiform, this displacement is dextral and sinistral, respectively. Shear sense analyses included both outcrop/hand specimen and microscopic scale observation (Tables 1 and 2). We also investigated microstructural evidence for different deformation mechanisms (and thus conditions) related to thrust and normal sense displacement (Table 3; cf. Vernon, 1989; Shelley, 1993; Passchier and Trouw, 1996; van der Pluijm and Marshak, 1997; and references therein).

The shearing we observed is clearly related to N–S stretching lineations defined by the same minerals as the main amphibolite-grade foliation parallel to the MMT. Phenomena associated with the large-scale antiform (rapid exhumation, decompression and leucogranites in the NPHM core) are of Neogene age (Chamberlain et al., 1989; Winslow et al., 1996). Cooling age datasets for several mineral systems all young towards the massif core (e.g. Treloar et al., 1991a,b, 2000; Whittington 1997; Schneider et al., 1999a; Schneider et al., 2001), suggesting that the eastern margin has been only weakly affected by the recent exhumation. Excess argon affects a few samples (George and Bartlett 1996; Reddy et al., 1997; Treloar et al., 2000), generally in local zones of high strain/fluid flux rather than pervasively throughout the eastern margin section.

Our data are from the eastern limb of the governing

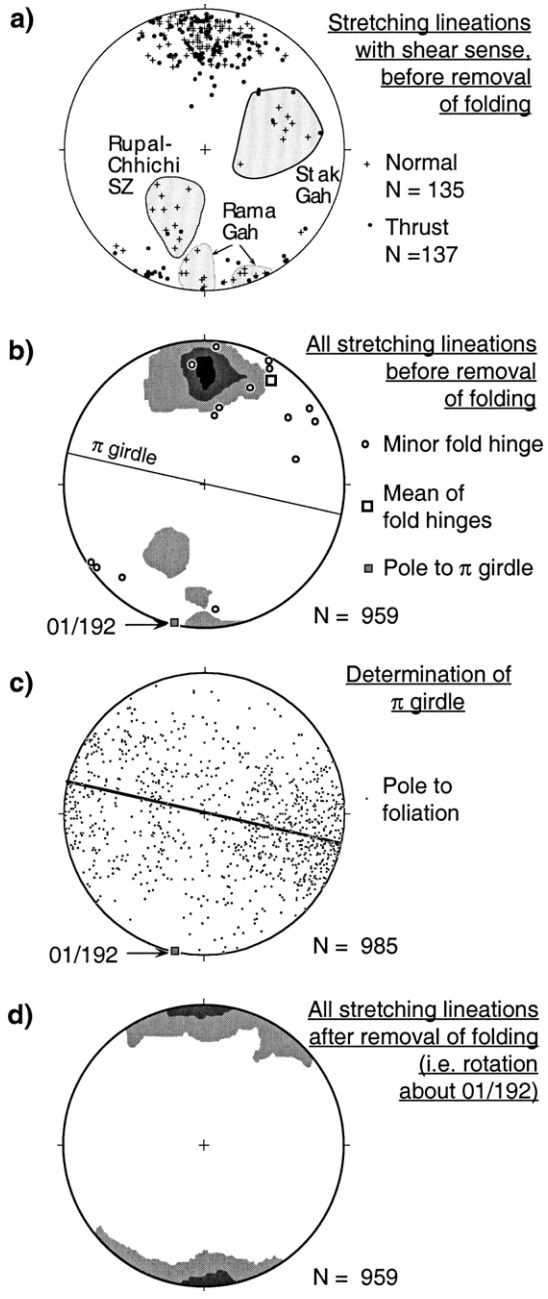

Fig. 6. Equal-area, lower hemisphere stereographic projections summarising the structure of the NPHM. All stereograms were plotted using the program Stereonet, version 4.9 (Allmendinger, 1995). N = number of data points in each case. Contour intervals are 2σ, with the default for a uniform point distribution set to 3σ and the first contour at 2σ; weight of shading is proportional to distribution density of data points. Details of the method can be found in the stereonet manual (Allmendinger, 1995). (a) Scatter plot showing stretching lineations from the eastern margin of the NPHM (including Stak Gah) as measured in the field. Only those lineation data where shear sense was determined are plotted, to discriminate lineations associated with inferred thrusting from lineations associated with inferred normal motion. Shaded fields highlight anomalies: those in Rama Gah and the Rupal–Chhichi Nala shear zone are associated with later deformation (<10 Ma) related to the rapid uplift of Nanga Parbat summit, while most lineations in Stak Gah show NE–SW trends, regardless of shear sense. Most of the lineation data, for both shear senses, have N–S trends. (b) 1% contour plot of all stretching lineation data for the NPHM, showing the dominant N–S trend, with minor fold hinges (open circles) plotted for comparison. The π girdle calculated from all NPHM foliation data (see part (c)) is also shown, along with the pole to the π girdle. (c) Scatter plot of all foliation data for NPHM, with matching π girdle as in part (b). Foliations are predominately steep and N–S striking. The pole to the girdle (01/192) is the rotation axis used for unfolding the stretching lineation data (see part (d)). (d) 1% contour plot of all stretching lineation data for the NPHM after removing the effect of the NPHM antiform (i.e. 'unfolding'). The restoration initially involved correction for the overall plunge of the NPHM antiform (1° towards an azimuth of 192, determined by the π girdle method, see part (c)), followed by unfolding of each foliation to the horizontal along with its corresponding lineation. The resulting distribution indicates that, prior to large-scale folding in the syntaxis, stretching lineations were dominantly N–S trending.

antiform, except near Harchu village where small subareas of inverted observed shear sense (i.e. dextral indicating original normal sense) coincide with the western limbs of the Dichil and Burdish Ridge antiforms. This coincidence itself lends further support, but is not crucial, to our contention that this folding postdated the shearing. We advocate caution, however, in extending this methodology further into the massif core, which is dominated by monotonous orthogneisses whose structure is a poorly-constrained composite of original Precambrian fabrics modified to varying degrees by the Neogene exhumation and high-grade metamorphism, including high-strain shear zones relating to the exhumation of Nanga Parbat itself (Schneider et al., 1999a; Butler et al., 2000).

5.2. State of strain and deformation conditions

The majority of the rocks in the SE NPHM are highly strained or mylonitic. In Fig. 4 we have discriminated low grade, outer NPHM rocks (originally Indian plate upper cover rocks) from higher-grade (±migmatitic) gneisses present further west at lower structural levels. A discontinuous Kfs–Grt megacrystic orthogneiss (the Rama Gneiss, formerly 'lath unit' (Edwards, 1998; Argles 2000; Edwards et al., 2000)) crops out between the low and high grade sections, a situation mirrored in the SW NPHM (Edwards et al., 2000). The division above is purely lithological, conferring no particular tectonostratigraphic significance (cf. Whittington et al., 1999). Only localities with unambiguous, non-coaxial kinematic indicators (e.g. asymmetric porphyroblast systems) are presented here; we omit outcrops dominated by conjugate shear sense indicators that we interpret as indicating nearly pure shear.

The lower grade metapelitic schists, marbles, and amphibolites are typically well foliated with strong N–S stretching lineations. Sense of shear indicators (see Table 1) include asymmetric, pre-or syn-tectonic porphyroblast systems (e.g. Fig. 8d), mica fish (Fig. 8c), *S–C* fabrics (also in some cases C'), shear bands and foliation boudinage structures, with discrete asymmetric shear zones in more competent lithologies (e.g. Fig. 7a and b). Some garnets have rotated >180° during growth, indicating significant non-coaxial shearing (see Vernon, 1989, and references within). Many isolated boudins of more competent layers

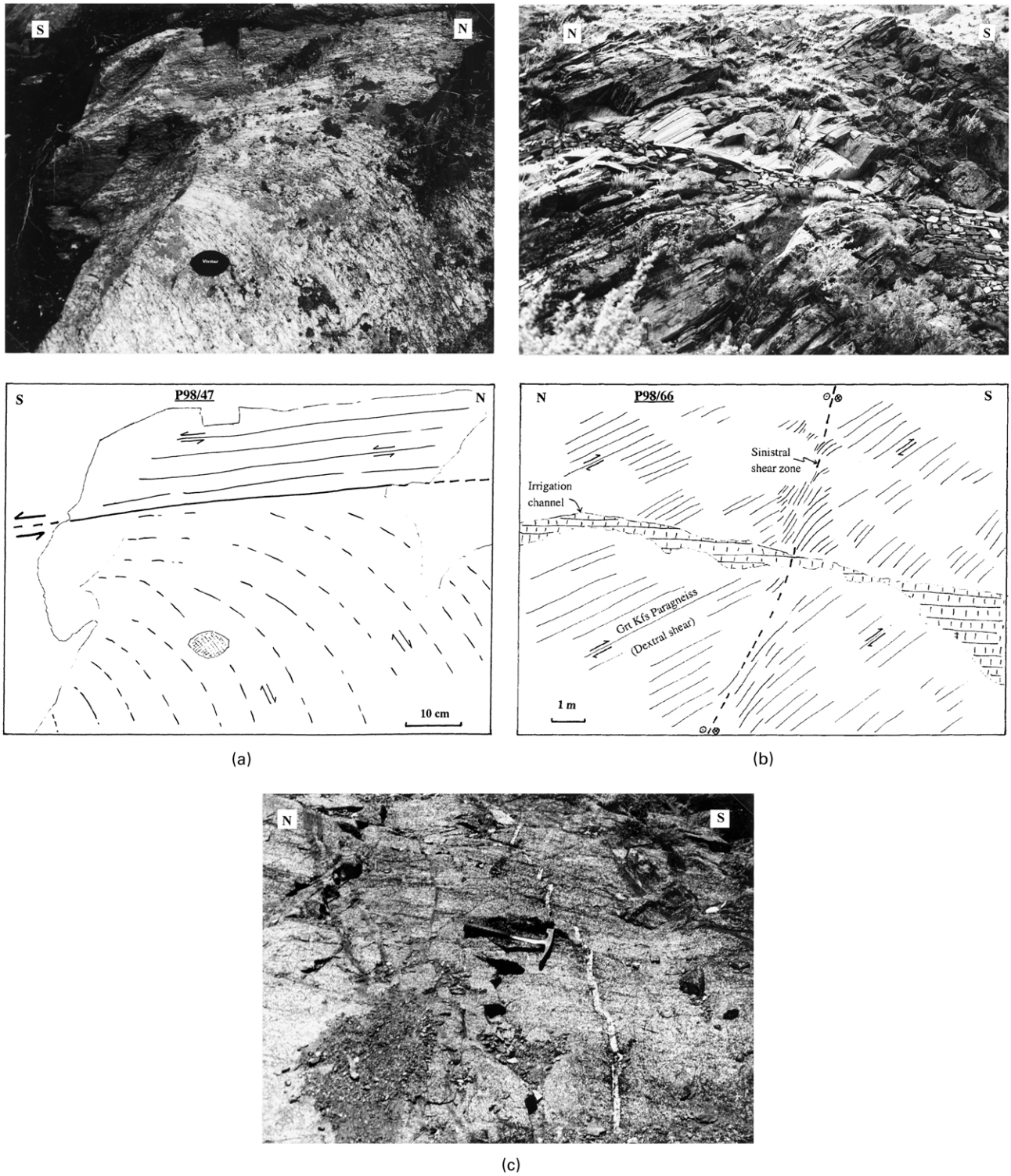

(e.g. amphibolites, calc-silicates) with an apparent sense of rotation and/or asymmetry were omitted unless corroborated by other indicators, as these structures are open to conflicting interpretation with regard to shear sense (e.g. Jordan, 1991, and references therein). Based upon deformation mechanisms deduced from microstructures, we estimate temperatures of deformation for the lower grade rocks to be ~300 to ~500°C (Table 3; e.g. Passchier and Trouw, 1996, and references therein, hereafter referenced as Table 3). In addition, thermobarometry on assemblages with original thrust shear sense gives consistently higher P–T conditions (ca. 550–650°C, 8–12 kbar) than those with original normal shear sense (ca. 490–550°C, 6–9 kbar) (Argles, 2000). This is consistent with normal shearing during the initial stages of cooling that just postdates thrusting at the metamorphic peak. Younger, brittle shear zones in

Table 1
Count of field localities and nature of shear sense criteria in the SE NPHM. A given criterion (e.g. Mica fish, *C/S* fabric, etc.) is counted when significantly well-developed (in either outcrop or thin-section). The numbers of localities where criteria occur are shown; a locality is defined as a section of rock where structural style and, broadly speaking, rock type are consistent. Localities may be exposures of 10–100 m across strike. Numerous localities where shear sense is completely ambiguous (e.g. conjugate structures) are not included; note also that some localities contain more than one criterion type. Figures in square brackets omit data from west of the hingeline of the Dichil antiform (where defined)

Shear sense	Criteria						
	Micafish	*S–C* fabric	Sigma/delta clasts/blasts	Shear bands	Boudin asymmetry	Shear zones[a]	Foliation boudinage[b]
Sinistral	7	9 [8]	42 [34]	8	3	6	2
Dextral	4	16 [14]	56 [47]	7	1	6 [4]	4 [2]
Both	–	–	3	1	–	4	–

[a] Ductile and discordant.
[b] Includes shear fractures.

the metapelites typically take up late cleavages and spaced fractures related to local, minor buckling and overturning.

The higher grade, mainly quartzo–feldspathic gneisses also preserve large strains (in a few cases prolate fabrics; $L \gg S$), though low strain zones occur, for example in the core of the Rama Gneiss—notwithstanding its Ordovician intrusion age (Foster et al., 1999). These gneisses preserve a slightly higher grade (terminology of Passchier and Trouw (1996)) of deformation than the metapelites to the west, including quartz ribbons, fine-grained quartz (typically with oblique grain shape fabric), incipient feldspar recrystallisation (core and mantle type textures; Fig. 8b), and well-developed trails from strong feldspar porphyroclasts. Rotated garnets are less common, as are mica fish or mica deflection in *S–C* fabrics. Estimated temperatures of deformation are ~450 to ~600°C (Table 3) and, as in the lower grade rocks, these are confirmed by geothermometry (Argles, 2000). The gneisses seem to have behaved more competently than the low-grade metapelites, as have the high-strain amphibolites of the KLS in the immediate hanging wall of the MMT. These show strong planar and linear fabrics, with some boudinage and tight folds, and uncommon, mainly ductile, shear sense indicators, though some systematic late shear fractures (e.g. Fig. 7c) also occur. Local chlorite-bearing schistose layers, remnants of supra-arc volcanogenic sediments (Pudsey, 1986; Searle, 1991), were intensely deformed under both ductile and brittle-ductile conditions at distinctly lower *P–T* conditions (524 ± 12°C, 8.3 kbar) than the other arc amphibolites (ca. 600–650°C, 8–11 kbar) (Argles, 2000).

5.3. Principal shear sense domains and overprinting relationships

Shear sense data in Fig. 4 are differentiated on observational (sinistral/dextral) and interpretational (normal/thrust) grounds, emphasising the correspondence of observed shear sense with kilometre-scale fold limbs (Fig. 3). Tables 1 and 2 present observed shear sense and overprinting relationship data by locality, relative to shear sense criteria (Table 1), and lithology (Table 2). Localities with crucial overprinting relationships are described in detail below, followed by a general summary of the dataset. We stress that in *all* cases of overprinting, inferred normal shearing overprints and thus post-dated inferred thrust-sense displacement fabrics.

1. Four occurrences (P98/47, 56, 106 and 116) show a consistent relationship: ductile, foliated gneiss with thrust-sense σ-type porphyroblast augen (Kfs, Grt) cut at a shallow angle by normal-sense, ductile, mylonitic shear zones. Localities 47, 106 and 116 occur in the marginal zone of the Rama gneiss, while 56 occurs in similar banded orthogneisses and paragneisses. Part of a typical shear zone at locality 47 is shown in Fig. 7a, and its microstructure in Fig. 8a to illustrate partial recovery (annealing). In the Stak valley (Fig. 2), outside the

Fig. 7. (a) Edge of sinistral mylonitic shear zone in the Rama gneiss, Bulan Gah (P98/47). Mylonitic foliation at top of view dips 40° WSW; the main outcrop surface is at a high angle to the foliation and inclined steeply towards the observer. Strain gradient can be estimated using the large K feldspar augen, lower left. Shear sense in the low-strain domains between shear zones is dextral on Kfs augen. Line drawing of the photograph included below, highlighting the salient features; note that the shear zone boundary is transitional, with the earlier foliation bending into the shear zone. (b) High-*T* sinistral, mylonitic shear zone in Grt Kfs paragneisses and leucogranites in the Stak valley, NE NPHM (P98/66; see Fig. 2). Shear zone runs almost vertically down the centre of the view, forming the gully in the lower half, and is best seen just above the irrigation channel wall. Foliation dips 40° ENE; photo looking up slope and roughly E. Shear sense on a gently NNW-plunging stretching lineation in the gneisses, within an already high-strain fabric, is dextral (from Grt and Kfs σ type porphyroblast systems). Shear zone shows sinistral motion, top-to-the-NW on a NW-plunging lineation. Line drawing of photograph, highlighting the sinistral shear zone for clarity. (c) High strain Ladakh Island Arc amphibolites, Gurikot Gah, (P97/81). Foliation dips 85° ENE; the outcrop surface shown is inclined gently towards the observer. No shear sense was observed in this outcrop on the main foliation, but all other KLS outcrops in the vicinity show dextral shear sense on the main foliation. A set of fine-grained, mafic veins (e.g. upper left to lower right) cut the foliation at a high angle, and deflection of ductile foliation at their margins also implies dextral shearing during their intrusion (or subsequent deformation). Both these mafic veins, and a suite of leucocratic veins (e.g. to right of hammer) are offset systematically by numerous foliation-parallel fractures demonstrating a sinistral shear sense.

Table 2
Summary of rock-types where shear sense was recorded. Rock-types represented by the localities in Table 1 (above). No locality is listed twice (i.e. no locality is repeated in the 'both' row). Note the tendency for dextral (mostly inferred thrust-sense) shear to be preserved in the rheologically stronger rock-types (amphibolite, pelitic gneiss and Rama gneiss), while sinistral (inferred normal) shear sense predominates in the weaker rheologies. The high proportion of sinistral shear in the orthogneisses reflects different structural domains in the interior of the massif (e.g. at Tarshing, Rama and west of Harchu), many of which are related to uplift of the massif core. Figures in square brackets omit data from west of the hingeline of the Dichil antiform (as in Table 1)

	Lithology				
Shear sense	Pelitic schist	Pelitic gneiss	Amphibolite	Orthogneiss	Rama gneiss
Sinistral	17	18 [9]	4	6 [4]	2
Dextral	10	29 [16]	6	5 [3]	3
Both	1	2 [1]	1	–	1

principal area we consider here, the same relationship (porphyroblast thrust fabric cut by normal ductile shear zones) was observed at five other localities in banded paragneisses. Several tourmaline leucogranite veins are associated with the shear zones; some show minor strain while others appear simply to exploit the shear zone trend, and are essentially undeformed. We do not further document this area here.

2. Locality P97/81 is in high-strain KLS amphibolites about 2 km E of the MMT in Gurikot Gah. The main foliation is the typically thrust MMT shear fabric. Later normal-sense displacement foliation-parallel mesofaults repeatedly offset both fine-grained mafic and leucocratic veins by a few centimetres with minor deflection of the adjacent foliation (Fig. 7c).
3. Cover schists at P97/78 (S of Harchu) show original thrust-sense shear for K-feldspar σ-type porphyroclast systems and a discrete shear fracture. These pre-date normal shear sense observed in thin section on garnet σ-type porphyroblasts and ductile shear bands.

From the above list, the clearest relationship is that of discrete, high-strain shear zones cross-cutting and deflecting an already relatively high-strain, penetrative tectonic fabric. The absolute consistency of shear sense is crucial: in all cases, the inferred normal-sense shear zones deform an

Table 3
Summary of temperature conditions inferred from deformation mechanisms based on microstructural observations of quartz and feldspar (e.g. Tullis and Yund, 1985, 1991; Vernon, 1989; Shelley, 1993; Passchier and Trouw, 1996; van der Pluijm and Marshak, 1997; and references therein). Shaded bars represent approximate temperature ranges for mechanisms (note the overlap in feldspar between brittle fracture and dislocation climb/glide processes at around 450–500°C. Static recrystallisation (e.g. of quartz ribbons in mylonites; Fig. 8a) appears common in the area, suggesting moderate–high temperatures persisted for some time after deformation. Microstructures indicating temperatures >600°C are rarely preserved in the SE NPHM (but see discussion concerning recovery in text)

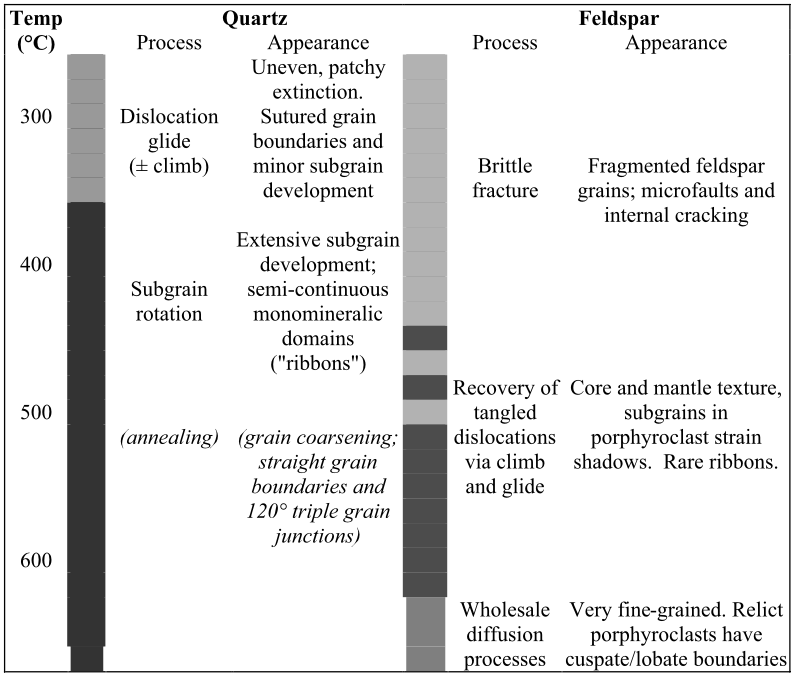

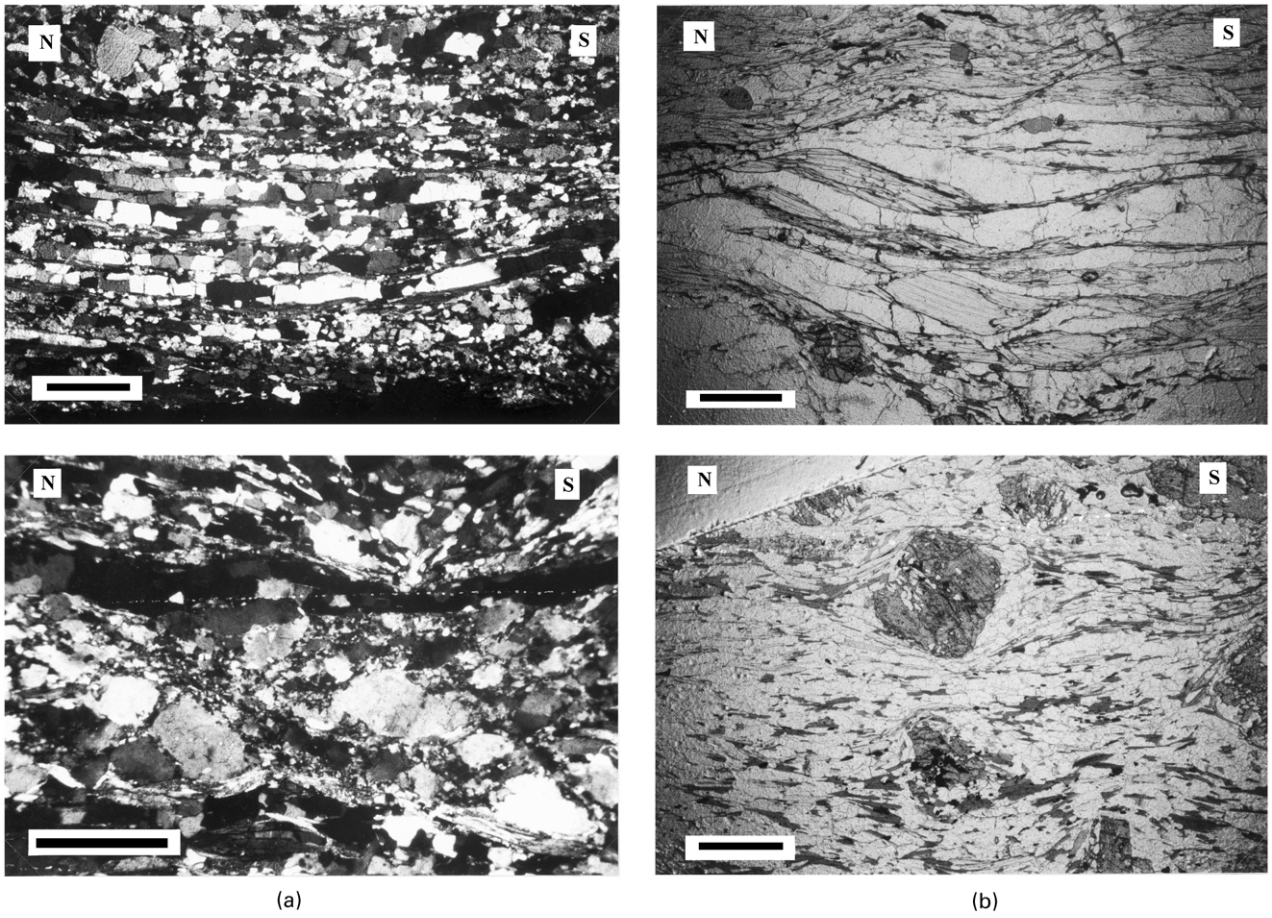

Fig. 8. (a) Optical photomicrograph of thin section cut from sample P98/47b, a high strain shear zone cutting the main foliation in the Rama gneiss, Bulan Gah left bank (see Fig. 4 for location). Aspect in field is protomylonitic (Fig. 7a). In plane polarised light the matrix is dominated by apparent quartz ribbons or bands. These 'ribbons' are the coarse-grained domains in the figure, with striking parallel-sided margins, but essentially polygonal internal microstructure. The bimodal grainsize of quartz in this sample could reflect either original grainsize differences or recovery of high-strain quartz ribbons (i.e. 'annealing'). Throughout the rock, muscovite and biotite in the high-strain fabric are coeval, emphasising the synmetamorphic nature of the deformation, and only locally do they delineate (i.e. 'pin') quartz ribbon boundaries. Section is cut parallel with lineation, perpendicular to foliation. Base of image is 7.5 mm. Crossed polars. (b) Optical photomicrograph of thin section P97/185b, high-strain shear zone in isolated gneissic outcrop, right bank of Chuggam valley (Fig. 4). Field aspect is protomylonitic, and shear sense was deduced from asymmetric trails on large feldspar clasts. Large feldspar clasts frequently show patchy extinction (microcracking), but also sutured internal grain boundaries indicating the onset of grain boundary migration and initiation of a 'core and mantle' type texture. Grain boundary migration and wholesale grain size reduction have operated extensively (both in field of view and elsewhere in thin section) as indicated by very fine (20–100 μm) grain size of surrounding quartzofeldspathic component. The occurrence of large (i.e. strong) feldspars deforming through grain boundary migration in a very fine grained matrix with quartz ribbons (now annealed as in Fig. 8a) suggests deformation possibly >500°C. Section is cut parallel with lineation. Base of image is 2.4 mm. Crossed polars. (c) Optical photomicrograph of thin section cut from sample P98/124b, a garnet micaschist approximately 500 m west of the MMT contact, right bank of the Astor river, just south of Harchu (Fig. 4). This garnet micaschist from the weak immediate footwall of the MMT shows abundant, synmetamorphic, original normal sense shear sense indicators. Characteristic structures are shown here, with large muscovite 'fish' and associated shear bands indicating direction of shear. Note the well-developed muscovite laths at the margins of the large mica fish (e.g. lower centre). Smaller biotite laths are concentrated at the rims of large muscovites, in a decompression texture typical to many samples in this zone; biotite also occurs along the shear bands. Much of the quartzofeldspathic matrix is coarse-grained, as in this view. We infer that extensive metamorphic re-working of the matrix occurred during the episode of normal (N-directed) shearing. In support of this hypothesis, kyanite and staurolite are absent from the matrix assemblage, although they occur as inclusions in garnet, suggesting that in the matrix they broke down during synmetamorphic deformation. Section is cut parallel with lineation, perpendicular to foliation; north is to the left. Base of image is 7.5 mm. Plane polarised light. (d) Optical photomicrograph of thin section cut from sample P97/168i, a garnet micaschist approximately 1 km west of the MMT contact on the left bank of the lower Rupal valley (Fig. 4). Sense of shear in this sample is normal, as indicated by asymmetric σ type garnet porphyroblast systems within an oblique muscovite–biotite foliation (slightly inclined from right to left, not parallel to the photograph margins). Because the microscope slide is overturned (facing upwards), the actual sense of shear is reversed; the apparent dextral/top-to-the-S shear sense is in reality sinistral/top-to-the-N when viewed down-dip. Note that the micas defining the asymmetry are recrystallised (polygonised) rather than simply bent, indicating synmetamorphic shear. In addition, the matrix is relatively coarse and close to polygonal, with many 120° triple junctions, despite the strong strain evident in the field. This suggests recovery of high-strain quartz microstructures, as discussed in the text. Section is cut parallel with lineation, perpendicular to foliation, and overturned. Base of image is 7.5 mm. Plane polarised light.

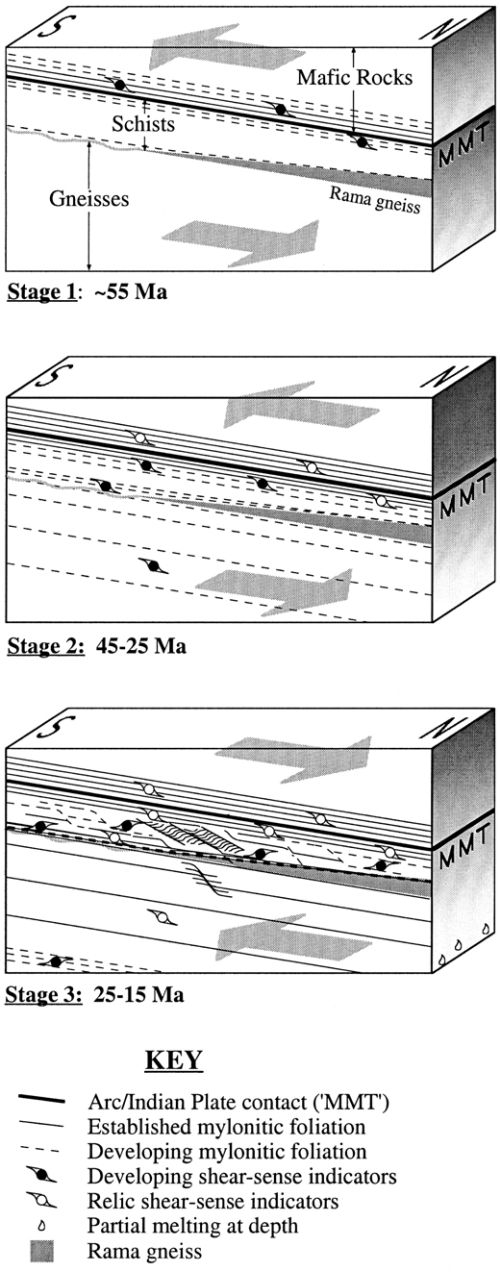

earlier, pervasive fabric characterised by inferred thrust-sense indicators. Normal displacement evidently occurred under ductile conditions not far below the metamorphic peak, since peak mineral assemblages remained stable in the mylonites (e.g. Table 3). At the same time, the strain partitioning in itself argues for deformation at slightly higher levels in the crust than the original, penetrative thrust-sense shearing. Direct dating of anatectic leucogranite veins in Stak valley that are associated with normal sense shear zones equivalent to those in the SE NPHM would provide a lower age limit on the normal-sense shearing. Similar leucogranites elsewhere in the NPHM are either Neogene (7–5 Ma) or early Miocene in age (Schneider et al., 1999b,c).

Locality 81 suggests that the relative timing of shear episodes observed in the footwall also pertains to the MMT hanging wall, but that the later, normal shearing occurred higher in the crust under less ductile conditions, and was of limited extent in the hanging wall. The only other instance of sinistral (inferred normal) shear indicators in the MMT hanging wall in this area is at localities P97/14 and 15 (Fig. 4). These extensively-reworked chlorite schists show ductile and brittle-ductile shear indicators (σ-type porphyroblasts, synmetamorphic pull-aparts in amphiboles). The dominance of normal shear here implies that they were preferentially exploited during this later shearing event as a weak horizon within the stronger hanging wall amphibolites—a theory supported by their relatively low recorded P–T conditions (see above).

Locality P97/78 presents the most confused picture, due mainly to poor timing constraints. Thrust displacement on the main fabric has been overprinted by normal shear bands, but as a variety of indicators suggest similar (near-peak) temperatures of deformation, the relationship is less clear. We suggest that this locality illustrates the variation of degrees of preservation and overprinting on all scales typical of the variably reworked lower-grade metapelites.

5.4. Summary of remaining shear-sense data from SE NHPM

There is a consistent pattern of shear sense distribution for much of the eastern margin. The few discernible non-coaxial strain indicators in mylonites along the MMT contact are all thrust-sense. Normal shear is most common in the schists to the west of the contact; isolated thrust-dominated outcrops occur in competent layers such as amphibolites, and ultimately dominate in the gneissic section further west. Both shear senses are preserved together, most commonly in the schist–gneiss transition

Fig. 9. Three stage model of fabric and shear feature development in the MMT zone. Front panel shows a cartoon of fabric evolution; side panel represents thermal structure of the section schematically. Motion is assumed N–S for simplicity. During Stage 1, initial southward thrusting of the arc over the Indian plate results in high strain along the contact. Deformation is partitioned into the relatively hot, ductile portion of the arc adjacent to the MMT. Presence and position of the Rama gneiss is conjectural. With continued southward thrusting in Stage 2, fabric development migrates downward into the footwall as these rocks heat up; at the same time the base of the arc cools, 'freezing in' early high-strain fabrics, and becoming rheologically resistant to further ductile deformation. Top-to-the-S indicators occur throughout the section. By the time northward extension begins, footwall temperatures have stabilised. Strain is partitioned into weak schists just below the MMT, and along the margins of the relatively competent Rama gneiss. The stronger underlying gneisses develop only some minor, discrete shear zones. The cool, mafic, strain-hardened base of the arc is not susceptible to this deformation; only rare, brittle-ductile N-directed shear structures form. With increased exhumation, heat is advected to shallow levels and shearing related to the uplift of Nanga Parbat occurs in the interior of the massif. Age data collated from Searle et al. (1987), Beck et al. (1995), Chamberlain and Zeitler (1996) and Foster et al. (2000).

zone (e.g. Bulan Gah, Gurikot Gah), showing the influence of rheology on the degree of overprinting. The Rama gneiss is an excellent illustration of this rheological partitioning, with discrete, discordant, normal-sense mylonite zones only at the margins of the body, while even thrust fabrics weaken towards the interior, implying this Ordovician granitoid resisted strain throughout the Himalayan orogeny, partitioning strain into its margins (Edwards, 1998; Argles, 2000). The zone of normal shear mirrors the schist-dominated section, widening southwards from 2 km in Bulan Gah to >5 km at Rattu.

From Rama Gah northwards to the Subsar Thrust (Argles, 2000), the only anomaly in the above pattern is that sinistral (inferred normal) shear dominates towards the interior of the massif, where kinematic indicators are sparse. This anomaly may result from lack of structural constraint (folding, northward extension of the Rupal–Chichi shear zone, preserved pre-Himalayan fabrics; Wheeler et al., 1995; Butler et al., 2000), even though observed shear sense changes as expected across the various mapped fold hinges (Figs. 3 and 4). Mylonites running N–S through Harchu may delineate the two shear sense domains, so that a consistent and retrodeformable pattern is only preserved east of Harchu. We are therefore reluctant to extend our hypothesis west of the area shown in Fig. 4.

6. Tectonic model

Fig. 9 presents a schematic model for the evolution of the MMT in the SE NPHM prior to syntaxial folding, which could apply more widely to sectors now overprinted by more recent tectonic events (e.g. the western margin of the NPHM; Butler et al., 1989). Note that the dates are a rough guide only, to place the model in the context of the current consensus on the timing of the Himalayan orogeny in N Pakistan; we address issues of timing further in the discussion.

In this qualitative model, it should be noted that the exposed footwall and hanging wall may have been finally juxtaposed only at a late stage, experiencing significantly different histories (e.g. at different crustal levels) up to that point. The major thrust shown is not the original, pre-collisional subduction zone; it certainly truncates the Kohistan–Ladakh arc stratigraphy on the western margin of the NPHM, and probably also on the eastern flank (e.g. Searle, 1991). It probably represents a 'break-back' thrust formed in the subduction zone hanging wall during collision, as suggested by Butler and Prior (1988). Stage 1 (Fig. 9a) of the model illustrates the initial phase of motion on this structure. High strain fabrics develop in the hanging wall at depth, but the currently-exposed footwall section remains less susceptible until thermal relaxation takes effect once thrusting slows or ceases. Another variable is the thermal state of the arc crust at this time. The lower portions may have been relatively hot during initial thrusting, augmented perhaps by dissipative shear heating (cf. Treloar, 1997), affording the potential for heat transfer from hot hanging wall to cold footwall (e.g. Royden, 1993; Ruppel and Hodges, 1994). Footwall strain is partitioned into discrete horizons, exploiting rheological contrasts (e.g. Rama gneiss margin), or is concentrated in the uppermost, high-strain levels, especially if an inverted thermal gradient develops (England and Molnar, 1993; Treloar, 1997). S-directed thrust sense features form predominately in the hanging wall. During the next stage (Fig. 9b), with continued underthrusting, the presently-exposed hanging wall cools (as in 'subduction refrigeration'; Peacock 1987), tending to 'freeze in' earlier high-strain fabrics and S-directed shear-sense indicators. The strong planar fabric combined with the rheological strength of the mafic hanging wall rocks partitions subsequent strain into the footwall of the Main Mantle Thrust. At the same time, discrete portions of the footwall begin to heat up, as they are buried to progressively deeper levels. This heating could be enhanced by a number of processes: localisation of material rich in radioactive elements (TARM; Jamieson et al., 1998; Huerta et al., 1999) either in the MMT zone, or in the MMT footwall by duplex formation (e.g. Coward et al., 1988; Treloar et al., 1989; Edwards et al., 2000); shear heating in the MMT zone (e.g. Molnar and England, 1990) and heat advection by fluid (or melt) transfer either intrusively or tectonically (Swapp and Hollister, 1991) from deeper levels in the shear zone. This heating would be further aided by the 'thermal reflectivity' of the low-conductivity mafic hanging wall (Treloar, 1997), causing 'heat focussing' (Jaupart and Provost, 1985). Stage 3 (Fig. 9c) marks the change from S-directed thrusting to N-directed normal motion in the present footwall of the MMT. This switch could be due to a number of factors: decrease in convergence rate, may be related to locking-up of the subduction zone; 'backsliding' on the original MMT (cf. Burg et al., 1984; but at deeper crustal levels); or extensional shearing along the top of an extruding buoyant tectonic body following either slab detachment (Chemenda et al., 2000) or initiation of another major thrust fault to the south (e.g. Hodges et al., 1993; Grujic et al., 1996; Dèzes et al., 1999; Grasemann and Vannay, 1999). Subsequent N-directed shearing is partitioned into the footwall, exploiting the weakest rheological horizons. The hanging wall amphibolites record the kinematics of this phase only in brittle or brittle-ductile features. With continued N-directed shearing and footwall exhumation, increased partitioning and development of brittle-ductile features occurs in the footwall. That these features are not widespread in the NPHM suggests the footwall rocks here record extension at a deeper level than those near Besham (Vince and Treloar, 1996), and this is consistent with numerous studies proposing that the NPHM has experienced significant uplift and exhumation in the last 10 Ma (e.g. Zeitler, 1985; Zeitler et al., 1989). Recent isotopic work in the NPHM (Whittington et al., 2000) has demonstrated that the core of the massif has a Lesser Himalayan

isotopic signature while the eastern margin corresponds to the High Himalayan unit, and thus the NPHM is correlatable with the rest of the orogen, albeit representing deeper structural levels. This work also suggests the eastern margin represents a highly condensed, if not significantly excised, section focused in the HHCS (cf. Argles, 2000), consistent with significant layer-parallel extension (e.g. Herren, 1987; Patel et al., 1993; Argles et al., 1999). Further studies (Foster and Argles, in preparation) will better constrain the position of this extensional zone in the NPHM section relative to the main orogen. However, we note that the basic data presented here are not inconsistent with models for extrusion of the HHCS (references above), and that our observations of sinistral (normal) shear overprinting dextral (thrust-sense) fabrics find parallels in studies of the STDS (e.g. Patel et al., 1993).

7. Discussion

7.1. Recovery of microstructures

Grain coarsening, both during and after high strain, has occurred in a number of the rocks studied, so that the mylonitic aspect of rocks in the field is not reflected in their microstructures (compare sample P98/47 in Figs. 7a and 8a). Many samples belie their complex tectonic history, however, with relatively simple matrix fabrics and shear sense indicators; earlier foliations (early Himalayan or, in some cases possibly pre-Himalayan) are entirely confined to the interiors of garnet porphyroblasts. Samples preserving thrust shear indicators appear little affected by subsequent strain, although there is some evidence for recovery and coarsening of quartz. In contrast, matrix textures in normal sense samples show abundant evidence of synmetamorphic recrystallisation (e.g. polygonized micas; Fig. 8d), in many cases being entirely reworked but for the most robust porphyroblast phases. Again, generally coarse quartz indicates a combination of metamorphic growth and recovery, belying the high-strain field aspect of the rocks. Hydrolytic weakening (e.g. Post et al., 1996) may have contributed to the re-working of the schists as opposed to the gneisses, which show evidence of reduced water activity during Himalayan metamorphism due to their prior metamorphism in the Precambrian (e.g. Powell, 1983). Despite these complications, we regard the main observation of thrust displacement, overprinted by normal-sense displacement in rheologically weak horizons, as sound.

7.2. MMT lineation trends

A broad consensus has emerged on original thrusting directions on the MMT near the NPHM (Treloar et al., 1991b; Butler et al., 1992; Wheeler et al., 1995; Argles, 2000; Butler et al., 2000; DiPietro et al., 2000; Edwards et al., 2000). This study supports the S- or SSE-directed thrusting direction inferred by other workers: stretching lineations trend predominately N–S on generally steep foliations, but there is no systematic change in trend in the few areas of shallower foliation dips (or after unfolding of the main antiform; Fig. 6). This implies that the original thrusting direction was close to due south except perhaps in the area between Stak La and Dichil Gali, where foliation strike and lineation trends swing NE, possibly related to the Subsar Thrust (Argles, 2000), or an original deviation in the MMT such as a lateral or oblique ramp. In the studied areas, lineations in rocks showing sinistral shear-sense indicators do not deviate significantly from the regional N–S trend. We therefore suggest that the hanging wall motion was N-directed during this extensional phase.

We have not attempted to unravel the more complex structures in the massif core where lineation trends vary considerably, for instance across shear zones associated with the recent uplift of Nanga Parbat (Edwards, 1998). It is likely that some lineations of variable orientation in lower strain regions within the syntaxis core may relate to earlier deformation (e.g. initial SW- and SE-directed thrusting seen west of the syntaxis (DiPietro et al., 2000), or even pre-Himalayan deformation (Butler et al., 2000)).

7.3. Amount and timing of excision

In contrast to examples of proven extensional excision (e.g. Davis, 1983; Norton, 1986; Argles et al., 1999), ductile shear fabrics along the eastern margin of the NPHM show minimal brittle overprinting, implying relatively high temperatures during and after deformation. If extension ceased while the rocks were still at moderate temperatures (ca. 500°C) in the middle crust, any metamorphic break formed would quickly become less distinct, and easily erased during subsequent fluid-present re-equilibration of the mineral assemblages and chemistries at these lower P–T conditions. Preliminary thermobarometry on the highly-condensed eastern margin section (Argles, 2000) indicates that normal shearing took place at slightly lower P–T conditions than thrusting, notwithstanding the polymetamorphic nature of the rocks and variety of lithologies. Apparent breaks in metamorphic grade between basement and cover rocks, or between medium-grade and low-grade cover schists, probably relate as much to juxtaposition of different lithotectonic units (Whittington et al., 2000) as to excision across extensional shear zones.

Significant exhumation of the leading edge of the Indian plate in the northwest Himalaya is required by exposures of high pressure assemblages formed at around 49 Ma (Tonarini et al., 1993) following collision. High pressure rocks also occur in the Stak valley (Pognante et al., 1993; Le Fort et al., 1997), and the discovery of coesite in eclogites near Babusar (O'Brien et al., 2001) confirms the magnitude of the exhumation. Peak metamorphic pressures in the NPHM (8–13 kbar (Pognante et al., 1993); 9–14 kbar (Argles, 2000)) were attained around 44–38 Ma (prograde

garnet growth; Foster et al., 2000), giving an upper age limit for initiation of extension. Geochronology elsewhere (near Babusar; Chamberlain et al., 1991) indicate several kilometres of normal motion based upon cooling curve discrepancies between >40 and 20 Ma. Burg et al. (1996) obtained a minimum of 5 km of vertical displacement based upon calculations of collapse folding during extension. Vince and Treloar (1996) described ductile to brittle extensional fabrics in the MMT footwall from E of Besham, and constrained the end of this N-directed shearing to 18 ± 2 Ma using apatite fission track data across the MMT. Earlier work (Treloar and Rex, 1990) suggested that a period of rapid cooling of ca. 8 My duration in the late Oligocene to early Miocene was at least partly related to extensional exhumation. The structural studies above document extension occurring at low grades (greenschist facies and below), mainly in the brittle regime. Preliminary P–T estimates from the southeastern NPHM on samples reworked during the normal shearing episode (Argles, 2000) give temperatures of 500–600°C at 7–9 kbar. Since deeper crustal levels are exposed within the NPHM, we suggest that the normal-sense features documented here represent a deeper expression of the same extension phase at the leading edge of the Indian plate, rather than a separate extensional episode. The recent model of Chemenda et al. (2000) postulates an extensional shear zone at depth involved in the rapid exhumation of high-pressure material soon after collision, and it is interesting to note that this zone occupies the same structural position (immediately south of the suture) as our zone of normal shear in the NPHM. Cooling age data in the southern NPHM imply a period of relatively slow cooling between hornblende (500°C; ~30–40 Ma) and mica (350–250°C; <10 Ma) Ar–Ar closure (George, 1993; Winslow et al., 1996; Whittington, 1997; Treloar et al., 2000), subject to fluid-derived excess argon effects (e.g. Reddy et al., 1997) and instability during step-heating (Gaber et al., 1988). The hornblende age could represent a lower limit for our period of tectonic exhumation, with slower cooling after extension ceased, but further work is needed to constrain the cooling paths more rigorously.

8. Conclusions

1. We observe a sinistral shear overprint on dextral shear fabrics on the eastern margin of the NPHM, which we interpret as N-directed, normal-sense displacement associated with mid-crustal extension following collision-related southward thrusting on the MMT. This is the first such record of medium–high grade extension from the NW Himalaya.
2. Extensional strain was partitioned mainly into the rheologically weak schists in the immediate footwall of the MMT, part of a highly condensed section including both High and Lesser Himalayan rocks.
3. Extensional structures overprint (postdate) S-directed MMT thrust fabrics, and we tentatively correlate the phase of extension with a widespread episode during the late Oligocene to early Miocene well-documented in the region.
4. Deeper levels of the original Himalayan thrust stack are exposed in the NPHM than in most of the NW Himalaya, providing a glimpse of mid-crustal processes during the initial stages of orogenic collapse.

Acknowledgements

This paper arose from the fusion of two datasets resulting from independent projects. MAE was supported by a USA National Science Foundation grant, and thanks Aslam Mohammad (deceased), Akhtar Karim (deceased), Anton Seimon, and Mitchel Wemple for logistic support, and W.S.F. Kidd, A. Pêcher, L. Seeber and D.A. Schneider for discussions. TWA was in receipt of a NERC Research Fellowship, and thanks Asif Khan, Mubarik Ali, Asghar Shah and Khush Jan for their help in Pakistan, and G.L. Foster and N.B.W. Harris for discussions. The authors acknowledge reviews from B. Grasemann, John Wheeler, an anonymous reviewer and J.-P. Burg that were instrumental in improving the finished article.

References

Allmendinger, R.W., 1995. Stereonet: a plotting program for orientation data for the Macintosh™ Computer.

Argles, T.W., 2000. The Evolution of the Main Mantle Thrust in the Western Syntaxis. In: Khan, M.A., Jan, M.Q., Treloar, P.J., Searle, M.P. (Eds.), Tectonics of Nanga Parbat and the Western Himalaya. Geological Society Special Publication 170, pp. 101–122.

Argles, T.W., Platt, J.P., Waters, D.J., 1999. Attenuation and Excision of a Crustal Section During Extensional Exhumation: The Carratraca Massif, Betic Cordillera, Southern Spain. Journal of the Geological Society of London 156, 149–162.

Bard, J.P., 1983. Metamorphism of an obducted island arc: an example of the Kohistan sequence (Pakistan) in the Himalaya collided range. Earth and Planetary Science Letters 65, 133–144.

Beck, R.A., Burbank, D.W., Sercombe, W.J., Riley, G.W., Barndt, J.K., Berry, J.R., Afzal, J., Khan, A.M., Jurgen, H., Metje, J., Cheema, A., Shafique, N.A., Lawrence, R.D., Khan, M.A., 1995. Stratigraphic evidence for an early collision between Northwest India and Asia. Nature 373, 55–58.

Burchfiel, B.C., Chen, Z., Hodges, K.V., Liu, Y., Royden, L.H., Deng, C., Xu, J., 1992. The South Tibetan detachment system, Himalayan orogen: Extension contemporaneous with and parallel to shortening in a collisional mountain belt. Geological Society of America Special Paper 269, 1–41.

Burg, J.-P., 1987. Regional shear variation in relation to diapirism and folding. Journal of Structural Geology 9 (8), 925–934.

Burg, J.P., Brunel, M., Gapais, D., Chen, G.M., Liu, G.H., 1984. Deformation of leucogranites of the crystalline Main Central Sheet in southern Tibet (China). Journal of Structural Geology 6, 535–542.

Burg, J.P., Chaudry, M.N., Ghazanfar, M., Anczkiewicz, R., Spencer, D., 1996. Structural evidence for back sliding of the Kohistan arc in the collisional system of northwest Pakistan. Geology 24 (8), 739–742.

Butler, R.W.H., Prior, D.J., 1988. Anatomy of a continental subduction zone: the main mantle thrust in Northern Pakistan. Geologische Rundschau 77 (1), 239–255.

Butler, R.W.H., Prior, D.J., Knipe, R.J., 1989. Neotectonics of the Nanga Parbat Syntaxis, Pakistan, and crustal stacking in the northwest Himalayas. Earth and Planetary Science Letters 94, 329–343.

Butler, R.W.H., George, M., Harris, N.B.W., Jones, C., Prior, D.J., Treloar, P.J., Wheeler, J., 1992. Geology of the northern part of the Nanga Parbat massif, northern Pakistan, and its implications for Himalayan tectonics. Journal of the Geological Society of London 149, 557–567.

Butler, R.W.H., Harris, N.W.B., Whittington, A.G., 1997. Interactions between deformation, magmatism and hydrothermal activity during active crustal thickening: a field example from Nanga Parbat, Pakistan Himalayas. Mineralogical Magazine 61, 37–52.

Butler, R.W.H., Wheeler, J., Treloar, P.J., Jones, C., 2000. Geological structure of the southern part of the Nanga Parbat massif, Pakistan Himalaya, and its tectonic implications. In: Khan, M.A., Jan, M.Q., Treloar, P.J., Searle, M.P. (Eds.), Tectonics of Nanga Parbat and the Western Himalaya. Geological Society Special Publication 170, pp. 123–136.

Chamberlain, P.C., Zeitler, P.K., 1996. Assembly of the crystalline terranes of the northwestern Himalaya and Karakoram, northwestern Pakistan. In: Yin, A., Harrison, M. (Eds.). The Tectonic Evolution of Asia. Cambridge University Press, pp. 138–148.

Chamberlain, C.P., Zeitler, P.K., Jan, M.Q., 1989. The dynamics of the suture between the Kohistan island arc and the Indian plate in the Himalaya of Pakistan. Journal of Metamorphic Geology 7, 135–149.

Chamberlain, C.P., Zeitler, P.K., Erickson, E., 1991. Constraints on the tectonic evolution of the northwestern Himalaya from geochronologic and petrologic studies of Babusar Pass, Pakistan. Journal of Geology 99, 829–849.

Chaudhry, M.N., Ghazanfar, M., 1987. Geology, structure and geomorphology of the Upper Kaghan valley, northwest Himalaya, Pakistan. Geological Bulletin of Punjab University 22, 13–57.

Chaudhry, M.N., Ghazanfar, M., 1990. Position of the Main Central Thrust in the tectonic framework of the Western Himalaya. Tectonophysics 174, 321–329.

Chemenda, A.I., Burg, J.-P., Mattauer, M., 2000. Evolutionary model of the Himalaya–Tibet system: geopoem based on new modelling, geological and geophysical data. Earth and Planetary Science Letters 174, 397–409.

Coward, M.P., 1985. A section through the Nanga Parbat syntaxis, Indus valley, Kohistan. Geological Bulletin of the University of Peshawar 18, 147–152.

Coward, M.P., Windley, B.F., Broughton, R.D., Luff, I.W., Petterson, M.G., Pudsey, C.J., Rex, D.C., Khan, M.A., 1986. Collision tectonics in the NW Himalayas. In: Coward, M.P., Ries, A.C. (Eds.), Collision Tectonics. Geological Society Special Publication 19, pp. 203–219.

Coward, M.P., Butler, R.W.H., Chambers, A.F., Graham, R.H., Izatt, C.N., Khan, M.A., Knipe, R.J., Prior, D.J., Treloar, P.J., Williams, M.P., 1988. Folding and imbrication of the Indian crust during Himalayan collision. Philosophical Transactions of the Royal Society of London A326, 89–116.

Craw, D., Koons, P.O., Winslow, D.M., Chamberlain, C.P., Zeitler, P.K., 1994. Boiling fluids in a region of rapid uplift, Nanga Parbat massif, Pakistan. Earth and Planetary Science Letters 128, 169–182.

Davis, G.H., 1983. Shear-zone model for the origin of metamorphic core complexes. Geology 11, 63–90.

Dèzes, P.J., Vannay, J.C., Steck, A., Bussy, F., Cosca, M., 1999. Synorogenic extension; quantitative constraints on the age and displacement of the Zanskar shear zone (Northwest Himalaya). Geological Society of America Bulletin 111 (3), 364–374.

DiPietro, J., Hussain, A., Ahmad, I., Khan, M.A., 2000. The Main Mantle Thrust in Pakistan: Its Character and Extent. In: Khan, M.A., Jan, M.Q., Treloar, P.J., Searle, M.P. (Eds.), Tectonics of Nanga Parbat and the Western Himalaya. Geological Society Special Publication 170, pp. 375–393.

Dixon, J.M., 1975. Finite strain and progressive deformation in models of diapiric structures. Tectonophysics 28, 89–124.

Edwards, M.A., 1998. Examples of tectonic mechanisms for local contraction and exhumation of the leading edge of India. Southern Tibet (28–29°N, 89–91°E) and Nanga Parbat, Pakistan. Ph.D. Thesis, State University of New York at Albany.

Edwards, M.A., Kidd, W.S.F., Li, J., Yue, Y., Clark, M., 1996. Multi stage development of the southern Tibetan detachment system near Khula Kangri. New data from Gonto La. Tectonophysics 260, 1–20.

Edwards, M.A., Kidd, W.S.F., Khan, M.A., Schneider, D.A., 2000. Tectonics of the SW Margin of the Nanga–Parbat Haramosh Massif. In: Khan, M.A., Jan, M.Q., Treloar, P.J., Searle, M.P. (Eds.), Tectonics of Nanga Parbat and the Western Himalaya. Geological Society Special Publication 170, pp. 77–100.

England, P.C., Molnar, P., 1993. The interpretation of inverted metamorphic isograds using simple physical calculations. Tectonophysics 12, 145–157.

Fielding, E.J., Isacks, M.J., Baranzangi, M., Duncan, C., 1994. How flat is Tibet? Geology 22, 163–166.

Foster, G.L., Argles, T.W., The pre-Himalayan magmatic and metamorphic history of the Nanga Parbat-Haramosh Massif, Pakistan. Manuscript in preparation.

Foster, G.L., Kinny, P., Vance, D., Harris, N., Argles, T., Whittington, A., 1999. The Pre-Tertiary Metamorphic History of the Nanga Parbat Haramosh Massif, Pakistan Himalaya. In: Sobel, E., Appel, E., Strecker, M., Ratschbacher, L., Blisniuk, P. (Eds.). Abstract volume of the 14th Himalaya–Tibet–Karakoram Workshop, 99/2. Terra Nostra, Kloster Ettal, Germany, pp. 44–45.

Foster, G., Kinny, P., Vance, D., Prince, C., Harris, N., 2000. The significance of monazite U–Th–Pb age data in metamorphic assemblages: a combined study of monazite and garnet chronometry. Earth and Planetary Science Letters 181, 327–340.

Gaber, L.J., Foland, K.A., Corbato, C.E., 1988. On the significance of argon release from biotite and amphibole during $^{40}Ar/^{39}Ar$ vacuum step heating. Geochimica et Cosmochimica Acta 52, 2457–2465.

Gansser, A., 1964. The Geology of the Himalayas. Interscience Publishers, New York.

Gansser, A., 1981. The geodynamic history of the Himalaya. In: Gupta, H.K., Delany, F.M. (Eds.), Zagros, Hindu Kush, Himalaya geodynamic evolution. American Geophysical Union Geodynamics Series 3, pp. 111–121.

George, M.T., 1993. The magmatic, thermal and exhumation history of the Nanga Parbat–Haramosh Massif, western Himalaya. Unpublished Ph.D. Thesis, Open University, Milton Keynes, UK.

George, M.T., Bartlett, J.M., 1996. Rejuvenation of Rb-Sr mica ages during shearing on the northwestern margin of the Nanga Parbat-Haramosh Massif. Tectonophysics 260, 167–185.

Grasemann, B., Vannay, J.C., 1999. Flow controlled inverted metamorphism in shear zones. Journal of Structural Geology 21 (7), 743–750.

Greco, A., Spencer, D.A., 1993. A section through the Indian plate, Kaghan Valley, NW Himalaya, Pakistan. In: Treloar, P.J., Searle, M.P. (Eds.), Himalayan Tectonics. Geological Society Special Publication 74, pp. 221–236.

Greco, A., Martinotti, G., Papritz, K., Ramsay, J.G., Rey, R., 1989. The Himalayan crystalline nappes of the Kaghan Valley (NE Pakistan). Eclogae Geologicae Helvetiae 82 (2), 629–653.

Grujic, D., Casey, M., Davidson, C., Hollister, L.S., Kündig, R., Pavlis, T., Schmid, S., 1996. Ductile extrusion of the Higher Himalayan Crystalline in Bhutan: evidence from quartz microfabrics. Tectonophysics 260, 21–43.

Guillot, S., de Sigoyer, J., Lardeaux, J.M., Mascle, G., 1997. Eclogitic metasediments from the Tso Morari area (Ladakh, Himalaya): evidence for continental subduction during India–Asia convergence. Contributions to Mineralogy and Petrology 128, 197–212.

Herren, E., 1987. Zanskar shear zone: Northeast–southwest extension within the Higher Himalayas (Ladakh, India). Geology 15, 409–413.

Hodges, K.V., Burchfiel, B.C., Royden, L.H., Chen, Z., Liu, Y., 1993. The

metamorphic signature of contemporaneous extension and shortening in the central Himalayan orogen: data from Nyalam transect, southern Tibet. Journal of Metamorphic Geology 11, 721–737.

Huerta, A.D., Royden, L.H., Hodges, K.V., 1999. The effects of accretion, erosion and radiogenic heat on the metamorphic evolution of collisional orogens. Journal of Metamorphic Geology 17 (4), 349–366.

Jamieson, R.A., Beaumont, C., Fullsack, P., Lee, B., 1998. Barrovian regional metamorphism; where's the heat? In: Treloar, P.J., O'Brien, P.J. (Eds.), What drives metamorphism and metamorphic reactions? Geological Society Special Publication 138, pp. 23–51.

Jaupart, C., Provost, A., 1985. Heat focussing, granite genesis and inverted metamorphic gradients in continental collision zones. Earth and Planetary Science Letters 73 (2-4), 385–397.

Jordan, P.G., 1991. Development of asymmetric shale pull-aparts in evaporite shear zones. Journal of Structural Geology 13 (4), 399–409.

Lawrence, R.D., Schroder, J.F., 1984. Active fault northwest of Nanga Parbat. In: Congress Secretariat (Ed.). Pakistan Geological Congress, Lahore, Pakistan. Institute of Geology, Punjab University.

Le Fort, P., Guillot, S., Pêcher, A., 1997. HP metamorphic belt along the Indus suture zone of NW Himalaya: new discoveries and significance. Comptes Rendus de l'Academie des Sciences 325, 773–778.

Lemennicier, Y., Le Fort, P., Lombardo, B., Pêcher, A., Rolfo, F., 1996. Tectonometamorphic evolution of the central Karakoram (Baltistan, northern Pakistan). Tectonophysics 260, 119–143.

Madin, I.P., 1986. Structure and neotectonics of the northwestern Nanga Parbat–Haramosh massif. Unpublished MSc. thesis, Oregon State University.

Madin, I.P., Lawrence, R.D., Ur-Rehman, S., 1989. The northwest Nanga Parbat–Haramosh Massif; evidence for crustal uplift at the northwestern corner of the Indian craton. Geological Society of America Special Paper 232, 169–182.

Molnar, P., England, P.C., 1990. Temperatures, heat flux, and frictional stress near major thrust faults. Journal of Geophysical Research 95 (4), 4833–4856.

Norton, M.G., 1986. Late Caledonian extension in western Norway: a response to extreme crustal thickening. Tectonics 5, 195–204.

O'Brien, P.J., Zotov, N., Law, R., Khan, M.A., Jan, M.Q., 2001. Coesite in Himalayan eclogite and implications for models of India–Asia collision. Geology 29 (5), 435–438.

Owen, L.A., 1989. Neotectonics and glacial deformation in the Karakoram mountains and the Nanga Parbat Himalaya. Tectonophysics 163, 227–265.

Passchier, C.W., Trouw, R.A.J., 1996. Microtectonics. Springer, Berlin, Heidelberg.

Patel, R.C., Singh, S., Asokan, A., Manickavasagam, R.M., Jain, A.K., 1993. Extensional tectonics in the Himalayan orogen, Zanskar, NW India. In: Treloar, P.J., Searle, M.P. (Eds.), Himalayan Tectonics. Geological Society Special Publication 74, pp. 445–459.

Peacock, S.M., 1987. Creation and preservation of subduction-related inverted metamorphic gradients. Journal of Geophysical Research 92, 12763–12781.

Pêcher, A., 1991. The contact between the higher Himalayan crystalline sediments and the Tibetan sedimentary series: Miocene large-scale dextral shearing. Tectonics 10, 587–598.

Pêcher, A., Le Fort, P., 1998. Late Miocene evolution of the Karakorum–Nanga Parbat contact zone (northern Pakistan). In: Macfarlane, A., Sorkhabi, R.B., Quade, J. (Eds.), Proceedings of the 11th Himalayan–Karakoram–Tibet Workshop, Geological Society of America Special Paper 328, pp. 145–158.

Pognante, U., Spencer, D.A., 1991. First report of eclogites from the Himalayan belt, Kaghan valley, Northern Pakistan. European Journal of Mineralogy 3, 613–618.

Pognante, U., Benna, P., Le Fort, P., 1993. High-pressure metamorphism in the High Himalayan Crystallines of the Stak valley, north-eastern Nanga Parbat–Haramosh syntaxis, Pakistan Himalaya. In: Treloar, P.J., Searle, M.P. (Eds.), Himalayan Tectonics. Geological Society Special Publication 74, pp. 161–172.

Post, A.D., Tullis, J., Yund, R.A., 1996. Effects of chemical environment on dislocation creep of quartzite. Journal of Geophysical Research 101 (B10), 22143–22155.

Powell, R., 1983. Fluids and melting under upper amphibolite facies conditions. Journal of the Geological Society of London 140, 629–633.

Pudsey, C.J., 1986. The Northern Suture in Pakistan; margin of a Cretaceous Island Arc. Geological Magazine 123, 405–423.

Reddy, S.M., Kelley, S.P., Magennis, L., 1997. A Microstructural and argon laserprobe study of shear zone development at the western margin of the Nanga Parbat–Haramosh Massif, Western Himalaya. Contributions to Mineralogy and Petrology 128, 16–29.

Royden, L., 1993. The tectonic expression of slab pull at continental convergent plate boundaries. Tectonics 12, 303–325.

Ruppel, C., Hodges, K.V., 1994. Pressure-temperature-time paths from two-dimensional thermal models; prograde, retrograde, and inverted metamorphism. Tectonics 13 (1), 17–44.

Schneider, D.A., Edwards, M.A., Kidd, W.S.F., Khan, M.A., Seeber, L., Zeitler, P.K., 1999a. Tectonics of Nanga Parbat, western Himalaya: Synkinematic plutonism within the doubly vergent shear zones of a crustal-scale pop-up structure. Geology 27 (11), 999–1002.

Schneider, D.A., Edwards, M.A., Zeitler, P.K., Coath, C.D., 1999b. Mazeno Pass Pluton and Jutial Pluton, Pakistan Himalaya: age and implications for entrapment mechanisms of two granites in the Himalaya. Contributions to Mineralogy and Petrology 136, 273–284.

Schneider, D.A., Kidd, W.S.F., Zeitler, P.K., Coath, C.D., 1999c. Early Miocene anatexis identified in the western syntaxis, Pakistan Himalaya. Earth and Planetary Science Letters 167, 121–129.

Schneider, D.A., Zeitler, P.K., Kidd, W.S.F., Edwards, M.A., 2001. Geochronologic constraints on the tectonic evolution and exhumation of Nanga Parbat, western Himalaya syntaxis, revisited. Journal of Geology 109, 563–583.

Searle, M.P., 1991. Geological Map of the Central Karakoram Mountains, Scale 1:250,000. In: Geology and Tectonics of the Karakorum Mountains, J. Wiley & Sons.

Searle, M.P., Windley, B.F., Coward, M.P., Cooper, D.J.W., Rex, A.J., Rex, D.C., Li, T., Xuchang, X., Jan, M.Q., Thakur, V.C., Kumar, S., 1987. The closing of Tethys and the tectonics of the Himalayas. Geological Society of America Bulletin 98, 678–701.

Searle, M.P., Cooper, D.J.W., Rex, A.J., 1988. Collision tectonics of the Ladakh–Zanskar Himalaya. Philosophical Transactions of the Royal Society of London A326, 117–150.

Seeber, L., Pêcher, A., 1998. Strain partitioning along the Himalayan arc and the Nanga Parbat antiform. Geology 26 (9), 791–794.

Shelley, D., 1993. Igneous and Metamorphic Rocks under the Microscope. 1st ed. Chapman & Hall, London.

Smith, H.A., Chamberlain, C.P., Zeitler, P.K., 1992. Documentation of Neogene regional metamorphism in the Himalayas of Pakistan using U–Pb in Monazite. Earth and Planetary Science Letters 113, 93–105.

Swapp, S.M., Hollister, L.S. 1991. Inverted metamorphism within the Tibetan slab of Bhutan; evidence for a tectonically transported heat-source. In: Gordon, T.M., Martin, R.F. (Eds.), Quantitative methods in petrology; an issue in honor of Hugh J Greenwood. Canadian Mineralogist 29, pp. 1019–1041.

Tahirkheli, R.A.K., Jan, M.Q., 1979. Geology of Kohistan and adjoining Eurasian and Indo-Pakistan continents, Pakistan. Geology of Kohistan 11 (1), 1–30.

Tonarini, S., Villa, I.M., Oberli, F., Meier, M., Spencer, D.A., Pognante, U., Ramsay, J.G., 1993. Eocene age of eclogite metamorphism in Pakistan Himalaya: implications for India–Eurasia collision. Terra Nova 5, 13–20.

Treloar, P.J., 1997. Thermal controls on early-Tertiary, short-lived, rapid regional metamorphism in the NW Himalaya, Pakistan. Tectonophysics 273, 77–104.

Treloar, P.J., Rex, D.C., 1990. Cooling and uplift histories of the crystalline thrust stack of the Indian plate internal zones west of Nanga Parbat, Pakistan Himalaya. Tectonophysics 180, 323–349.

Treloar, P.J., Broughton, R.D., Williams, M.P., Coward, M.P., Windley,

B.F., 1989. Deformation, metamorphism and imbrication of the Indian plate, south of the Main Mantle Thrust, north Pakistan. Journal of Metamorphic Geology 7, 111–125.

Treloar, P.J., Williams, M.P., Rex, D.C., 1991a. The role of erosion and extension in unroofing the Indian plate thrust stack, Pakistan Himalaya. Geological Magazine 128, 465–478.

Treloar, P.J., Potts, G.J., Wheeler, J., Rex, D.C., 1991b. Structural evolution and asymmetric uplift of the Nanga Parbat syntaxis, Pakistan Himalaya. Geologische Rundschau 80, 411–428.

Treloar, P.J., Rex, D.C., Guise, P.G., Wheeler, J., Hurford, A.J., Carter, A., 2000. Geochronological constraints on the evolution of the Nanga Parbat syntaxis, Pakistan Himalaya. In: Khan, M.A., Jan, M.Q., Treloar, P.J., Searle, M.P. (Eds.), Tectonics of Nanga Parbat and the Western Himalaya. Geological Society Special Publication, London 170, pp. 137–162.

Tullis, J., Yund, R.A., 1985. Dynamic recrystallisation of feldspar: a mechanism for ductile shear zone formation. Geology 13, 238–241.

Tullis, J., Yund, R.A., 1991. Diffusion creep in feldspar aggregates: experimental evidence. Journal of Structural Geology 13, 987–1000.

van der Pluijm, B., Marshak, S., 1997. Earth Structure—an Introduction to Structural Geology and Tectonics. WCM/McGraw-Hill.

Vernon, R.H., 1989. Porphyroblast-matrix microstructural relationships: recent approaches and problems. In: Daly, J.S., Cliff, R.A., Yardley, B.W.D. (Eds.), Evolution of Metamorphic Belts. Geological Society Special Publication 43, pp. 83–102.

Vince, K.J., Treloar, P.J., 1996. Miocene, north-vergent extensional displacements along the Main Mantle Thrust, NW Himalaya, Pakistan. Journal of the Geological Society of London 153, 677–680.

Wadia, D.N., 1931. The syntaxis of the northwest Himalaya, tectonics and orogeny. Records of the Geological Survey of India 65, 189–220.

Wadia, D.N., 1932. Note on the geology of Nanga Parbat (Mt. Diamir), and adjoining portions of Chilas, Gilgit district, Kashmir. Records of the Geological Survey of India 66, 212–234.

Wheeler, J., Treloar, P.J., Potts, G.J., 1995. Structural and metamorphic evolution of the Nanga Parbat syntaxis, Pakistan Himalayas, on the Indus gorge transect: the importance of early events. Geological Journal 30, 349–371.

Whittington, A.G., 1997. The thermal, metamorphic and magmatic evolution of a rapidly exhuming terrane: the Nanga Parbat Massif, northern Pakistan. Ph.D. thesis, Open University, Milton Keynes, UK.

Whittington, A.G., Harris, N.B.W., Ayres, M.W., Foster, G.L., 1999. Lithostratigraphic correlations in the western Himalaya —an isotopic approach. Geology 27 (7), 585–588.

Whittington, A.G., Harris, N.B.W., Ayres, M.W., Foster, G.L., 2000. Tracing the origins of the western Himalaya; an isotopic comparison of the Nanga Parbat massif and Zanskar Himalaya. In: Khan, M.A., Jan, M.Q., Treloar, P.J., Searle, M.P. (Eds.), Tectonics of the Nanga Parbat syntaxis and the western Himalaya. Geological Society Special Publication 170, pp. 201–218.

Winslow, D.M., Zeitler, P.K., Chamberlain, C.P., Williams, I.S., 1996. Geochronologic constraints on syntaxial development in the Nanga Parbat region, Pakistan. Tectonics 15 (6), 1292–1308.

Zeitler, P.K., 1985. Cooling history of the NW Himalaya, Pakistan. Tectonics 4, 127–151.

Zeitler, P.K., Sutter, J.F., Williams, I.S., Zartman, R., Tahirkheli, R.A.K., 1989. Geochronology and temperature history of the Nanga Parbat–Haramosh Massif, Pakistan. Geological Society of America Special Paper 232, 1–22.

Zeitler, P.K., Chamberlain, C.P., Smith, H.A., 1993. Synchronous anatexis, metamorphism, and rapid denudation at Nanga Parbat (Pakistan Himalaya). Geology 21, 347–350.